A single-column simulation of the GABLS arctic stable boundary layer intercomparison case using One-Dimensional Turbulence

Alan Kerstein and Scott Wunsch
Combustion Research Facility
Sandia National Laboratories, Livermore, CA 94551-0969

May 28, 2003

Abstract

One-Dimensional Turbulence (ODT) is a single-column simulation in which turbulent vertical transport is repesented by an unsteady advective process, rather than its customary representation by a diffusive process. The salient feature of ODT with reference to simulation of the atmospheric boundary layer (ABL) is that it resolves fine-grained unsteady motions and transport processes. The ODT representation of episodic turbulent bursts that occur under stongly stable conditions would be a promising topic for future research.

1 Introduction

One-Dimensional Turbulence (ODT) is a turbulence simulation model formulated on a one-dimensional (1D) spatial domain. In an ABL context, it is a form of single-column modeling. There are several important differences between ODT and other single-column models. Because of this, and because ODT has not previously been applied to ABL modeling, a brief description of the method and of results for the GABLS arctic stable boundary layer intercomparison case are provided here. The description is not intended to be self-contained because details are provided in cited publications.

In previous applications (but not in the present application), the 1D domain resolves molecular-transport processes (viscosity, heat transport, mass transport, etc.). Turbulent transport, which is usually modeled as a coarse-grained diffusive process, is represented in ODT by a random sequence of rearrangements (mathematically, mappings) applied to randomly selected intervals of the 1D domain. These

rearrangements may be viewed as the model analog of turbulent eddies, and are therefore termed eddies or eddy events.

The mapping that represents a turbulent eddy is defined so as to emulate the key attributes of turbulent eddies: overturning motion and compression that amplifies property gradients. It may be viewed as an idealization of the effect of a notional turbulent eddy on property profiles along a 1D line of sight.

The times of occurrence, locations, and spatial extents of eddy events in ODT are randomly sampled; the physics governing the spatiotemporal structure of turbulence is incorporated through the mathematical relations that determine the likelihood of particular eddy characteristics as a function of the instantaneous flow state. These relations are based on familiar, well established mixing-length phenomenology. This application of mixing-length concepts is closer in principle to the underlying physics than mixing-length applications to coarse-grained formulations involving spatial, temporal, or ensemble averaging. Though strictly speaking, the mixing-length relations used in ODT are parameterizations, their adherence to the physics governing local, time-resolved evolution results in a particularly simple, robust formulation involving minimal parameter adjustment. Numerous applications supporting this characterization have been reported in the literature, e.g., [1, 2, 3].

In Sec. 2, the ODT formulation applied here to the GABLS intercomparison case is briefly described. The description is intended to summarize the present formulation with emphasis on differences from previous formulations. A new feature is that molecular transport processes are not resolved in this application. Rather, viscosity is assigned a value that phenomenologically represents near-surface roughness effects. This assignment, an assumed value of the turbulent Prandtl number, and assignment of another parameter that controls the von Karman constant, are the only empirical inputs other than the physical setup and parameters specified for the intercomparison.

2 One-dimensional model

2.1 Time advancement

ODT single-column simulations of the ABL evolve vertical profiles of velocity components, u, v, and w, and potential temperature, θ. Each profile depends on time t and the vertical coordinate z. This evolution involves two processes: eddy events, causing instantaneous modifications of these profiles, and intervening time advancement of conventional form.

The time advancement between eddy events is governed by

$$\left(\partial_t - \nu\partial_z^2\right) u(z,t) = f\left(v(z,t) - V_g\right) \tag{1}$$

$$\left(\partial_t - \nu\partial_z^2\right) v(z,t) = -f\left(u(z,t) - U_g\right) \tag{2}$$

$$\left(\partial_t - \nu\partial_z^2\right) w(z,t) = 0 \tag{3}$$

$$\left(\partial_t - \gamma\partial_z^2\right) \theta(z,t) = 0. \tag{4}$$

Here ν is viscosity, γ is thermal diffusivity, f is the coriolis parameter, and U_g and V_g are the geostrophic winds. These equations are solved within a closed domain of height Λ. Boundary conditions applied to the velocity at the surface ($z = 0$) are $u(z = 0) = v(z = 0) = w(z = 0) = 0$ and at the top ($z = \Lambda$) are $u(z = \Lambda) = U_g$, $v(z = \Lambda) = V_g$, and $w(z = \Lambda) = 0$. As an initial condition, the potential temperature at the ground is $\theta(z = 0, t = 0) = \theta_o$. However, the ground temperature cools at a constant rate $\dot{\theta}_g$, so that the bottom boundary condition evolves as $\theta(z = 0, t) = \theta_o - \dot{\theta}_g t$. The potential temperature at the top is fixed at all times at $\theta(z = \Lambda) = \theta_o + \Delta\theta$. Parameter values, spatial resolution, and initial profiles for the intercomparison case are discussed in Secs. 2.4 and 3.

2.2 Eddy definition

The basic element of the model is the advective mapping. It consists of a measure-preserving map $M(z)$ of the domain onto itself, so that any scalar $\psi(z)$ undergoes the transformation $\psi(z) \to \psi(M(z))$ when acted on by the map. Measure-preservation, the one-dimensional equivalent of incompressibility, implies conservation of all scalars. The mapping acts on a segment of length l, from position z_o to $z_o + l$. The selection of values of z_o and l for a particular mapping is discussed in Sec. 2.3. (Here, z_o is an arbitrary height, not the roughness height introduced in Sec. 2.4.)

The mapping is loosely interpreted as representing the effects of a turbulent eddy of size l on the scalar fields in the corresponding z interval. All four scalar quantities are mapped to mimic the transport of fluid elements. The particular mapping function is arbitrary, but a piecewise-linear function is chosen as a convenient way to satisfy the requirements of measure-preservation and finite extent. As in all previous ODT work, a three-piece function which takes the line segment, shrinks it to a third of its original length, and then places three copies on the original domain, is used. The middle copy is reversed, so that the mapped field $\psi(M(z))$ is continuous if $\psi(z)$ is continuous. The mapping function reduces to the identity map $M(z) = z$ outside of the mapped interval.

The rearrangement of the potential-temperature field by the mapping alters the total potential energy, but the mapping itself leaves the total kinetic energy unchanged. To enforce energy conservation, a function of specified form is added to each velocity scalar whenever an eddy occurs. The fluid displacements induced by the mapping are $K(z) \equiv z - M(z)$; this is a natural candidate for the energy exchange function, and is mathematically convenient. This function is non-zero only within the mapped region. Under the action of an eddy, the potential temperature and velocity fields undergo the transformations

$$\theta(z) \to \theta(M(z)) \tag{5}$$

$$u(z) \rightarrow u(M(z)) + c_u K(z)$$
$$v(z) \rightarrow v(M(z)) + c_v K(z)$$
$$w(z) \rightarrow w(M(z)) + c_w K(z).$$

The amplitudes c_i of the energy exchange terms $c_i K(z)$ are determined for each eddy individually to achieve both total energy conservation and an exchange of energy among velocity components. The exchange of energy is the ODT implementation of the return-to-isotropy phenomenology that is commonly introduced in Reynolds-averaged models of turbulent shear flow. The incorporation of this phenomenology into ODT is discussed further in [1]. The use of the function $K(z)$ to enforce energy conservation in buoyant stratified flow was introduced in [2]. The present formulation uses $K(z)$ for both purposes, reflecting the combination of shear and buoyancy forcing that governs ABL evolution.

To calculate c_i, the procedure of [1] is generalized to include buoyancy. The energy-equipartition assumption ($\alpha = 1/3$ in the notation of that reference) is adopted in the energy-exchange submodel. The amplitudes are then

$$c_u = \frac{27}{4l}\left(-u_K \pm \sqrt{\frac{1}{3}\left(u_K^2 + v_K^2 + w_K^2 - \frac{8gl}{27}\frac{\theta_K}{T_o}\right)}\right) \tag{6}$$
$$c_v = \frac{27}{4l}\left(-v_K \pm \sqrt{\frac{1}{3}\left(u_K^2 + v_K^2 + w_K^2 - \frac{8gl}{27}\frac{\theta_K}{T_o}\right)}\right)$$
$$c_w = \frac{27}{4l}\left(-w_K \pm \sqrt{\frac{1}{3}\left(u_K^2 + v_K^2 + w_K^2 - \frac{8gl}{27}\frac{\theta_K}{T_o}\right)}\right)$$

where

$$s_K \equiv \frac{4}{9l^2}\int_{z_o}^{z_o+l} s(z)(l - 2(z - z_o))dz \tag{7}$$

is a function of any scalar field, and T_o is a reference potential temperature. Substitution of these constants into Eq. 5 results in conservation of the total energy, with equipartition of the available energy (defined in [1]) among the three velocity scalars.

2.3 Eddy selection

The final ingredient required in the model is a procedure to determine the time sequence of eddy events and the parameters z_o and l for each event. A statistical procedure is employed that involves random sampling from an eddy rate distribution, here assumed to be of the form

$$\lambda = \frac{C\nu}{l^4}\sqrt{\left(\frac{u_K l}{\nu}\right)^2 + \left(\frac{v_K l}{\nu}\right)^2 + \left(\frac{w_K l}{\nu}\right)^2 - \frac{8gl^3}{27\nu^2}\frac{\theta_K}{T_o} - Z}. \tag{8}$$

This expression involves two free parameters, C and Z, whose roles in the present context are explained in Sec. 2.4.

The cited references explain the physical motivation for the assumed form and way that this distribution is used to sample eddy events. Here it is noted that the argument of the square root is a quantity interpreted as a normalized measure of the total energy available to drive a particular eddy event, reduced by an amount Z whose role is explained in Sec. 2.4.

If two of the three velocity components are removed from the model, Eq. 8 reduces to the eddy rate distribution used in [2]. If the buoyancy term is omitted, Eq. 8 resembles the expression for λ that appears in [1], except that here, λ is based on the total available energy (including contributions from all three velocity components) rather than the available energy associated with vertical motion. Use of the total available energy is advantageous here because it gives the correct critical Richardson number. Another distinction from [1] is that the procedure that was used previously to suppress occasional unphysically large eddy events is omitted here. For the present application, the stable stratification suffices to prevent such anomalies.

2.4 Application to the ABL

Because molecular transport processes are negligible away from the near-surface region, it is unnecessary (and unaffordable, even in 1D) to resolve them throughout the vertical extent of the ABL. In fact, they need not be resolved near the surface either, because there they are dominated by roughness effects. Therefore the viscosity ν is used here as a free parameter that is adjusted to provide an empirical representation of surface roughness.

The adjustment is based on the near-surface boundary-layer structure that is resolved by ODT. If ν is taken to be the molecular viscosity, then the ODT simulation is a fully resolved representation of near-wall dynamics. If this representation is accurate, then the ODT mean velocity profile should capture the viscous, buffer, and log layers respectively. ODT simulations of channel and Couette flow do in fact reproduce this structure, and quantitatively accurate results are obtained by adjustment of the parameters C and Z in Eq. 8.

The empirical representation of roughness is based on the respective roles of C and Z in Eq. 8. Z determines a threshold Reynolds number for eddy turnover. (If the quantity under the square root is negative, the eddy event is disallowed.) In a boundary layer, Z controls the viscous suppression of near-wall eddies, and thus the extent of the buffer layer. C scales the overall event rate and thus the turbulence intensity. Therefore the choice of C directly affects turbulent transport in the log layer, and indirectly affects the viscous and buffer layers through the interactions among layers. The net effect is that the von Karman constant κ increases with increasing C.

In this context, roughness is modeled as a viscosity enhancement. Namely, the mean velocity $m = (\langle u \rangle^2 + \langle v \rangle^2)^{1/2}$ is required to obey viscous scaling, $m/u_* = z/z_*$,

from $z = 0$ to the roughness height z_0. (Here, u_* and z_* are based on $m(z)$ rather than $u(z)$, consistent with conventions specified for the intercomparison.) The viscosity ν is adjusted to satisfy this requirement. In this application, ν is thus an effective viscosity representing roughness effects rather than the molecular viscosity. (Implementation of this procedure for the intercomparison case is discussed in Sec. 3.1.) For the value $z_0 = 0.1$m used in the intercomparison, this height exceeds the extent of the buffer layer that would appear in the boundary layer above a flat wall, so it is assumed that buffer-layer effects are subsumed within the roughness-dominated region. For this reason, Z is set equal to zero. For Couette flow with $Z = 0$, ODT mean velocity profiles transition from viscous to log scaling over a short y_* interval, with no inflection point (in semilog coordinates). Log scaling with $\kappa = 0.4$ is obtained for $C = 0.93$. Accordingly, the parameter values $Z = 0$, $C = 0.93$ are used for ODT simulation of the intercomparison case.

The Prandtl number of air is 0.7. Turbulent heat transfer studies indicate that this is also a reasonable value for the turbulent Prandtl number, so γ in Eq. 4 is assigned the value $\nu/0.7$.

The initial and boundary conditions of the ODT simulation are as specified for the intercomparison, except that the initial u profile has a linear ramp from $z = 0$ to $z = 4$m to avoid possible numerical problems resulting from extremely high local shear near $z = 0$.

2.5 Non-dimensionalization

To render the ODT model in non-dimensional form for numerical simulation, it is necessary to rescale the length, time, velocity, and potential temperature variables by reference values. The obvious reference length scale is the domain height Λ. The dimensionless position z' and eddy size l' are defined by $z' \equiv z/\Lambda$ and $l' \equiv l/\Lambda$. Time is rescaled in terms of the time scale for viscous smoothing of domain-scale structures: $t' \equiv t\nu/\Lambda^2$. These choices result in dimensionless velocities that are like Reynolds numbers and a dimensionless gravity parameter that is like a Rayleigh number.

The velocities are defined in units of z'/t': $u' \equiv Cu\Lambda/\nu$, and likewise for v and w. The inclusion of C in the dimensionless velocity is shown below to collapse the parameter dependence of the non-dimensional formulation into a single term. The time evolution equation for the velocity fields become

$$\left(\frac{\partial}{\partial t'} - \frac{\partial^2}{\partial z'^2}\right) u' = f'\left(v' - V_g'\right) \tag{9}$$

$$\left(\frac{\partial}{\partial t'} - \frac{\partial^2}{\partial z'^2}\right) v' = -f'\left(u' - U_g'\right)$$

$$\left(\frac{\partial}{\partial t'} - \frac{\partial^2}{\partial z'^2}\right) w' = 0$$

where $f' \equiv \Lambda^2 f/\nu$ and $U_g' \equiv CU_g\Lambda/\nu$, etc. A dimensionless potential temperature is defined to vary between 0 and 1 initially:

$$\theta' \equiv \frac{(\theta - \theta_o)}{\Delta\theta}. \tag{10}$$

The dimensionless potential temperature evolves according to

$$\frac{\partial\theta'}{\partial t'} = \frac{1}{Pr}\frac{\partial^2\theta'}{\partial z'^2} \tag{11}$$

where $Pr \equiv \nu/\gamma$ is the Prandtl number. The boundary value at $z' = 0$ is given by $\theta'(0,t') = -\dot{\theta}'t'$ where $\dot{\theta}' \equiv \Lambda^2\dot{\theta}_g/\nu\Delta\theta$.

The rescaled eddy rate distribution is

$$\lambda' = \frac{1}{l'^4}\sqrt{(l'u_K')^2 + (l'v_K')^2 + (l'w_K')^2 - g'\theta_K' l'^3 - ZC^2} \tag{12}$$

where the dimensionless gravity is $g' \equiv \frac{8C^2\Delta\theta\Lambda^3}{27T_o\nu^2}g$. The dimensionless measure of velocity and density fluctuations is

$$s_K' \equiv \frac{4}{9l'^2}\int_{z_o'}^{z_o'+l'} dz' s'(z')(l' - 2(z' - z_o')). \tag{13}$$

where s denotes u, v, w, or θ. The ODT model now contains a single intrinsic parameter ZC^2, as well as the physical control parameters g', Pr, f', $\dot{\theta}'$, U_g', and V_g'. As noted in Sec. 2.4, Z and therefore ZC^2 are set equal to zero in the ABL application of ODT. C nevertheless affects the computed results for a given case (e.g., through the C dependence of κ) because C appears in the definition of dimensionless velocities.

3 Results for the intercomparison case

3.1 Viscosity adjustment

As explained in Sec. 2.4, the viscosity used in ODT simulation of the intercomparison case is chosen so that the mean horizontal velocity obeys viscous scaling, $m/u_* = z/z_*$, for $z \leq z_0$, where $z_0 = 0.1$m is the roughness height for the intercomparison case. For the ODT parameter values $C = 0.93$ and $Z = 0$ used to simulate this case (see Sec. 2.4), this condition is satisfied for $\nu = 0.02\text{m}^2/\text{s}$, which is therefore the viscosity value used for this application.

Figure 1 shows a portion of the wall-scaled mean velocity profile based on the last hour of simulation. To resolve the viscous layer sufficiently so that the numerical simulation closely approximates the continuum limit, a mesh spacing of 0.025m is used, requiring 16000 mesh points to span the 400m domain height. For larger ν, a

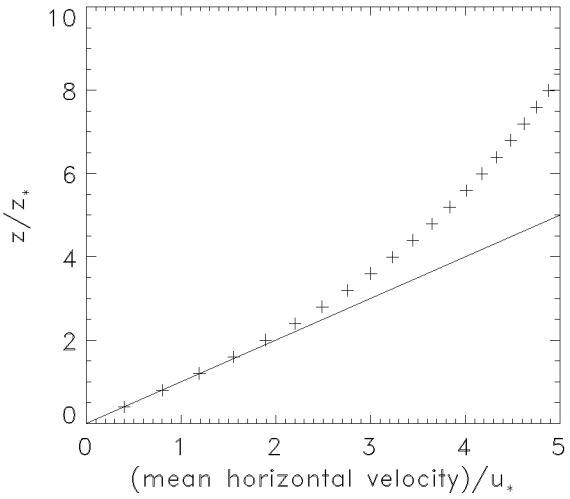

Figure 1: Near-wall mean horizontal velocity based on the final hour of simulation (+), compared to viscous scaling (solid).

coarser mesh would provide adequate resolution. In the present context, variation of ν would provide an indication of roughness-height sensitivity.

The plot demonstrates viscous scaling up to four mesh spacings above the surface, corresponding to the target value $z_0 = 0.1\text{m}$. The plot also indicates that the simulation resolves $z_* = 0.4$.

To assess the effect of running the simulation with larger ν on a coarser mesh, a case was run with $\nu = 1\text{m}^2/\text{s}$ on a 200-cell mesh. The ABL grew much too rapidly. For ν this large, viscous momentum transfer (in effect, eddy viscosity) dominates transport by ODT eddy events. ODT simulation on a mesh this coarse requires a more sophisticated determination of ν than simply assigning a constant value. Namely, low-resolution ODT simulation of the ABL would require an eddy-viscosity closure analogous to closures used in LES. Development of this approach would be a worthwhile undertaking but has not yet been pursued. Here, the choice $\nu = 0.02\text{m}^2/\text{s}$ has little apparent effect on simulated ABL evolution beyond the viscous layer, other than its essential role as the mechanism of kinetic-energy dissipation. For this ν value, velocity fluctuations are adequately resolved on the 16000-cell mesh. Thus, $\nu = 0.02\text{m}^2/\text{s}$ is sufficiently dissipative without contributing significantly to total transport (except in the near-wall region).

3.2 Mean profiles

The output files for the intercomparison provide the first two hundred points above $z = 0$ at full resolution (0.025m), and points above that averaged in groups of 100. All profiles shown here are averaged over the last hour of simulation.

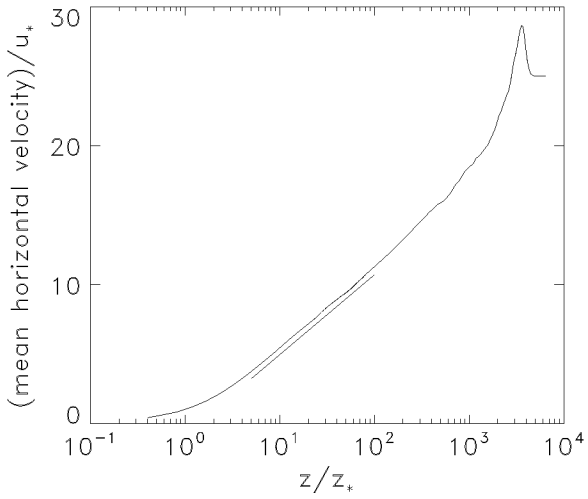

Figure 2: Mean horizontal velocity in wall coordinates (curve), compared to log scaling with $\kappa = 0.4$ (line segment).

Figure 2 shows the mean horizontal velocity plotted in wall coordinates. A line segment corresponding to log scaling with $\kappa = 0.4$ is shown for comparison. The short duration of the simulation and effects of transient evolution may cause the log scaling to be less precise than for simulations of statistically steady confined flows. Nevertheless, consistency with $\kappa = 0.4$ is apparent.

Figure 3 shows the vertical profile of the mean u velocity. The jet at the top of the ABL is evident. The velocity at the surface appears to be greater than zero because the near-wall high-gradient region is not discernible in this format. Models lacking the spatial resolution and/or physical mechanisms required to simulate the near-surface flow may not capture large near-surface increments of velocity and other properties.

The normalized Ekman spiral based on the mean velocities is shown in Figure 4 and the mean potential temperature is shown in Figure 5. Instantaneous profiles are are also shown in Figure 5 to illustrate structural variability during the simulations and to highlight the large near-surface gradients.

3.3 Fluctuation profiles

Vertical profiles of selected fluctuation statistics are shown in Figures 6-8. Despite the vertical binning over most of the domain (see Sec. 3.2), the profiles are noisy. This reflects the fact that the ODT is an unsteady simulation capturing individual eddy motions, like LES, but is 1D and therefore involves no horizontal averaging, like other SCMs. Despite the variability, precision is sufficient, as indicated by comparison to the previous averaging period (not shown here).

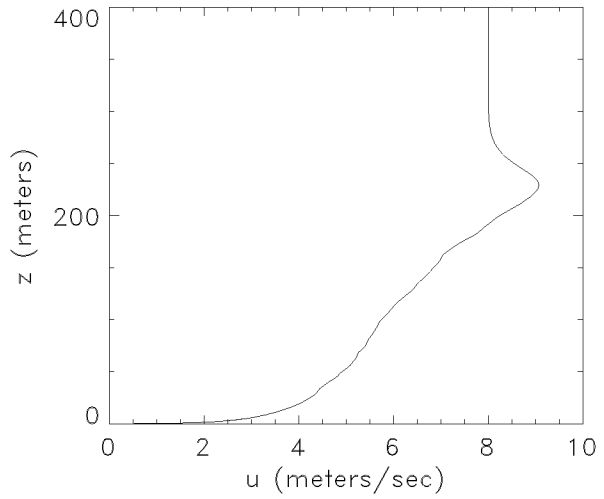

Figure 3: Vertical profile of mean u velocity.

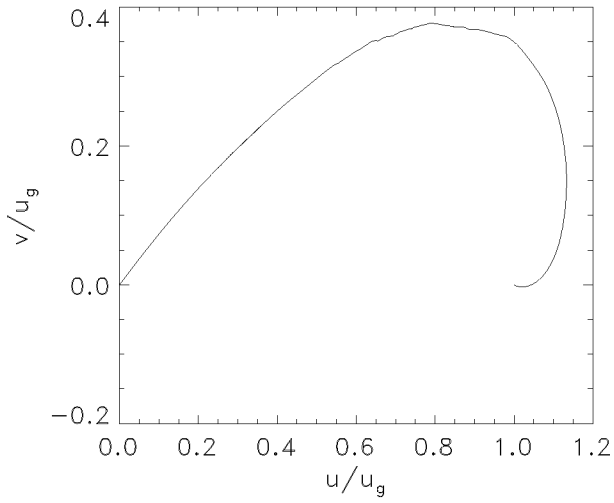

Figure 4: Normalized Ekman spiral.

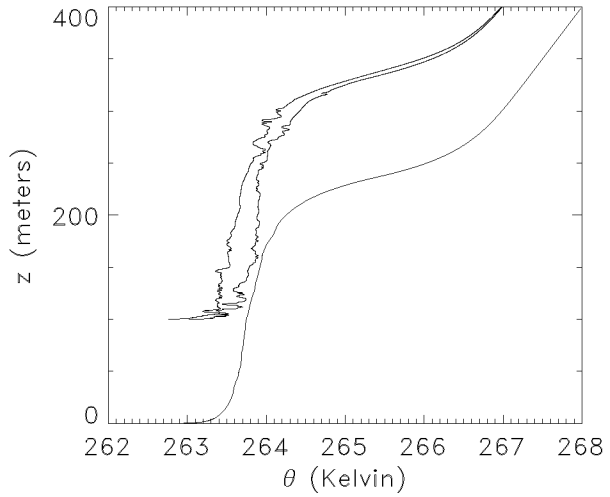

Figure 5: Vertical profiles of mean potential temperature and of instantaneous potential temperature at the beginning and end of the averaging period (displaced upward 100m).

The only property that is noise-dominated is total transport in Figure 8. Comparison to the previous averaging period and to test cases indicates that the vertical profile of total transport, gathered from a sufficiently large ensemble of simulated realizations, would be negligible compared to the dominant budget terms when plotted in this format.

Near the surface, fluctuations properties are similar to results previously reported for channel flow [3], with minor differences due to the differences in parameter values and in some details of the model formulation (Sec. 2). In particular, total transport is non-negligible near the wall but it is adequately resolved there. (One hour is sufficient averaging time for near-wall statistics because the time scale of the dominant near-wall eddies is shorter than than dominant time scale away from the wall.) The production and dissipation profiles attain much larger values (off scale in Figure 8) near the wall than in LES [4] because they transition in ODT from dependence on bulk parameters (u_* and f) to dependence on wall parameters (u_* and ν). The near-wall structure is physically correct, as indicated by previous [3] comparisons to direct-numerical-simulation results.

3.4 Data omissions

In the data files, vertical velocity skewness is omitted because ODT does not provide a physically correct representation of high-order vertical-velocity statistics. It nevertheless yields reasonable vertical fluxes (Figure 7) because these fluxes are based on advective motions occurring in ODT (eddy events) rather than the nominal vertical

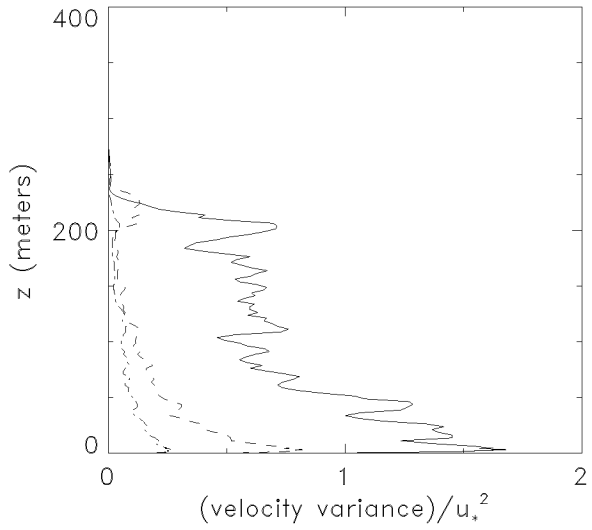

Figure 6: Velocity variances scaled by u_*^2: $\langle u^2 \rangle$ (solid), $\langle v^2 \rangle$ (dash), $\langle w^2 \rangle$ (dot-dash).

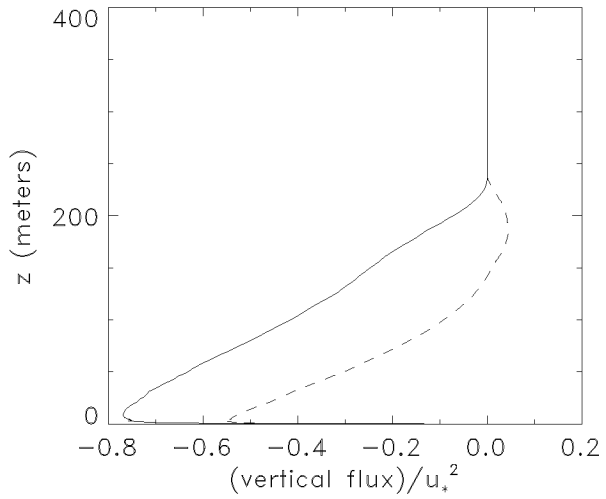

Figure 7: Vertical fluxes scaled by u_*^2: $\langle uw \rangle$ (solid), $\langle vw \rangle$ (dash).

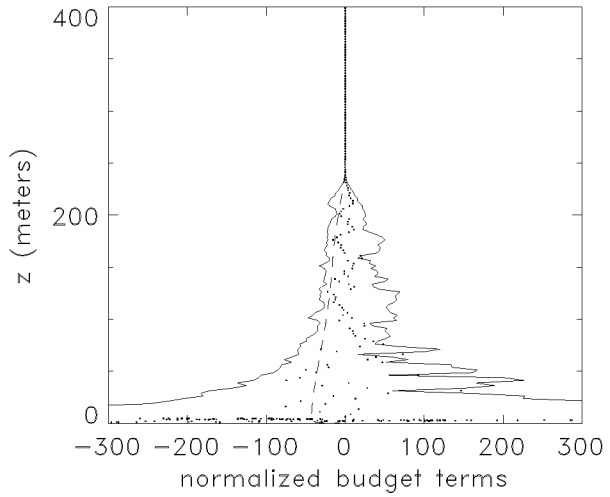

Figure 8: TKE budget terms scaled by $u_*^2 f$: production (solid; positive), dissipation (solid; negative), buoyant production (dash), total transport (points).

velocity profile, which does not advect fluid [1].

TKE storage is omitted because the TKE budget is obtained by assuming that the averaging period corresponds to statistically steady evolution, so by definition there is no time evolution of any statistical property. (There are neither horizontal coordinates nor, presently, an ensemble of realizations that would allow the time evolution of statistical properties to be quantified.)

The time-series file omits the boundary-layer height because this quantity has poor statistical properties in the absence of averaging over horizontal coordinates.

References

[1] W. Ashurst, A. R. Kerstein, S. Wunsch, and V. Nilsen, One-dimensional turbulence: vector formulation and application to free shear flows, *J. Fluid Mech.* **447**, 85-109 (2001).

[2] S. Wunsch and A. R. Kerstein, A model for layer formation in stably-stratified turbulence. *Phys. Fluids* **13**, 702-712 (2001).

[3] R. C. Schmidt, A. R. Kerstein, S. Wunsch, and V. Nilsen, Near-wall LES closure based on one-dimensional turbulence modeling, *J. Comp. Phys.* **186**, 317-355 (2003).

[4] Kosovic, B., and Curry, J., A large eddy simulation study of a quasy-steady, stably stratified atmospheric boundary layer. *J. Atmos. Sci.* **57**, 1052-1068 (2000).